

## Validating neural-network refinements of nuclear mass models

R. Utama<sup>\*</sup> and J. Piekarewicz<sup>†</sup>*Department of Physics, Florida State University, Tallahassee, Florida 32306, USA*

(Received 27 September 2017; published 16 January 2018)

**Background:** Nuclear astrophysics centers on the role of nuclear physics in the cosmos. In particular, nuclear masses at the limits of stability are critical in the development of stellar structure and the origin of the elements.

**Purpose:** We aim to test and validate the predictions of recently refined nuclear mass models against the newly published AME2016 compilation.

**Methods:** The basic paradigm underlining the recently refined nuclear mass models is based on existing state-of-the-art models that are subsequently refined through the training of an artificial neural network. Bayesian inference is used to determine the parameters of the neural network so that statistical uncertainties are provided for all model predictions.

**Results:** We observe a significant improvement in the Bayesian neural network (BNN) predictions relative to the corresponding “bare” models when compared to the nearly 50 new masses reported in the AME2016 compilation. Further, AME2016 estimates for the handful of impactful isotopes in the determination of  $r$ -process abundances are found to be in fairly good agreement with our theoretical predictions. Indeed, the BNN-improved Duflo-Zuker model predicts a root-mean-square deviation relative to experiment of  $\sigma_{\text{rms}} \simeq 400$  keV.

**Conclusions:** Given the excellent performance of the BNN refinement in confronting the recently published AME2016 compilation, we are confident of its critical role in our quest for mass models of the highest quality. Moreover, as uncertainty quantification is at the core of the BNN approach, the improved mass models are in a unique position to identify those nuclei that will have the strongest impact in resolving some of the outstanding questions in nuclear astrophysics.

DOI: [10.1103/PhysRevC.97.014306](https://doi.org/10.1103/PhysRevC.97.014306)

### I. INTRODUCTION

As articulated in the most recent U.S. long-range plan for nuclear science [1] “nuclear astrophysics addresses the role of nuclear physics in our universe,” particularly in the development of structure and on the origin of the chemical elements. In this context, fundamental nuclear properties such as masses, radii, and lifetimes play a critical role. However, knowledge of these nuclear properties is required at the extreme conditions of density, temperature, and isospin asymmetry found in most astrophysical environments. Indeed, exotic nuclei near the drip lines are at the core of several fundamental questions driving nuclear structure and astrophysics today: *What are the limits of nuclear binding? Where do the chemical elements come from? What is the nature of matter at extreme densities?* [1–3].

Although new experimental facilities have been commissioned with the aim of measuring nuclear masses, radii, and decays far away from stability, at present some of the required astrophysical inputs are still derived from often uncontrolled theoretical extrapolations. And even though modern experimental facilities of the highest intensity and longest reach will determine nuclear properties with unprecedented accuracy throughout the nuclear chart, it has been recognized that

many nuclei of astrophysical relevance will remain beyond the experimental reach [4–6]. Thus, reliance on theoretical models that extrapolate into unknown regions of the nuclear chart becomes unavoidable. Unfortunately, these extrapolations are highly uncertain and may ultimately lead to faulty conclusions [7]. However, one should not underestimate the vital role that experiments play and will continue to play. Indeed, measurements of even a handful of exotic short-lived isotopes are of critical importance in constraining theoretical models and in so doing better guide the extrapolations.

Whereas no clear-cut remedy exists to cure such unavoidable extrapolations, we have recently offered a path to mitigate the problem [6,8,9] primarily in the case of nuclear masses. The basic paradigm behind our two-pronged approach is to start with a robust underlying theoretical model that captures as much physics as possible followed by a *Bayesian neural network* (BNN) refinement that aims to account for the missing physics [6]. Several virtues were identified in such a combined approach. First, we observed a significant improvement in the predictions of those nuclear masses that were excluded from the training of the neural network—even for some of the most sophisticated mass models available in the literature [10–12]. Second, mass models of similar quality that differ widely in their predictions far away from stability tend to drastically and systematically reduce their theoretical spread after the implementation of the BNN refinement. Finally, due to the Bayesian nature of the approach, the refined predictions are always accompanied by statistical uncertainties. This philosophy was

<sup>\*</sup>Present address: Cold Spring Harbor Laboratory, Cold Spring Harbor, NY 11724; [utama@cshl.edu](mailto:utama@cshl.edu)

<sup>†</sup>[jpiekarewicz@fsu.edu](mailto:jpiekarewicz@fsu.edu)

adopted in our most recent work [9], which culminated with the publication of two refined mass models: the mic-mac model of Duflo and Zuker [11] and the microscopic HFB-19 functional of Goriely and collaborators [12]. Tables for the total binding energy, as well as neutron, and proton separation energies for these two newly published mass models are provided as supplemental material in Ref. [9].

Shortly after the submission of our latest manuscript [9] we became aware of the newly published atomic mass evaluation AME2016 [13]. This is highly relevant given that the training of the neural network relied exclusively on a previous mass compilation (AME2012) [14]. Thus, insofar as the nearly 50 new masses appearing in the newest compilation, ours are genuine theoretical predictions. Confronting the newly refined mass models against the newly published data is the main goal of this article.

This short manuscript has been organized as follows. First, no further physics justification nor detailed account of the BNN framework are given here, as both were extensively addressed in our most recent publication [9]. Second, the results presented in Sec. II are limited to those nuclei appearing in the AME2016 compilation whose masses were not reported previously or whose values, although determined from experimental trends of neighboring nuclides, have a strong impact on  $r$ -process nucleosynthesis. As we articulate below, the main outcome from this study is the validation of the novel BNN approach. Indeed, we conclude that the improvement reported in Ref. [9] extends to the newly determined nuclear masses—which in the present case represent true model predictions. We end the paper with a brief summary in Sec. III.

## II. RESULTS

Although the formalism has already been discussed in great detail in Sec. III of Ref. [9], we provide here a short synopsis of the most important details of the BNN framework. At the core of the BNN approach is a posterior probability distribution that is built from the product of a prior distribution of neural-network (NN) parameters times a likelihood that a given set of parameters describes the given experimental data. Note that the posterior distribution aims to improve *mass residuals* between the fairly accurate predictions of the original mass model and the experimental data. Whereas the construction of the likelihood is relatively straightforward, the prior probability requires the introduction of “hyperparameters.” To a large extent, the determination of the hyperparameters relies on assumptions that have been proven effective and reliable through mostly trial and error [15]. Hence, we assume as in Refs. [6,15] that all NN parameters are independent and use a Gaussian prior centered around zero and with a width controlled as discussed in Refs. [16,17]. Once the posterior distribution has been constructed, we adopt Markov chain Monte Carlo (MCMC) sampling to generate a faithful distribution of the NN parameters. In turn, such a distribution of NN parameters generates the corresponding probability distribution of mass residuals. In this manner reliable statistical estimates are provided for both the average and the variance of each mass residual.

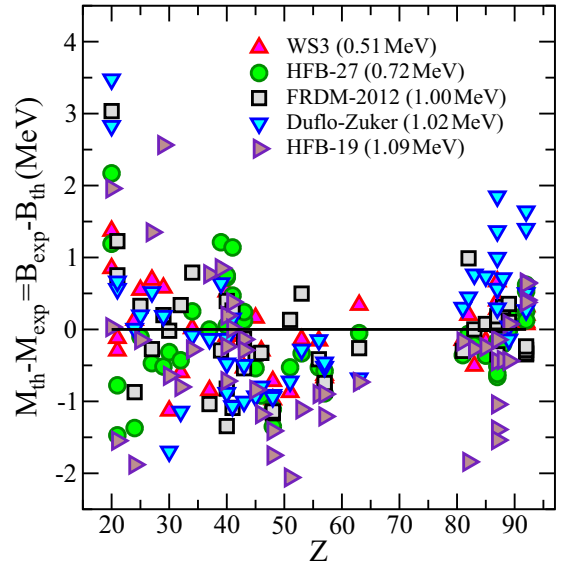


FIG. 1. Theoretical predictions for the total binding energy relative to experiment for the 46 nuclei in the  $^{40}\text{Ca}$ – $^{240}\text{U}$  region that appear in the latest AME2016 compilation but not in any of the earlier mass evaluations. The models shown here are representative of some of the most sophisticated mass models available in the literature. Quantities in parentheses denote the rms deviations.

In Ref. [9] we published refined mass tables with the aim of taming the unavoidable extrapolations into unexplored regions of the nuclear chart that are critical for astrophysical applications. Specifically, we refined the predictions of both the Duflo-Zuker [11] and HFB-19 [12] models using the AME2012 compilation in the mass region from  $^{40}\text{Ca}$  to  $^{240}\text{U}$ . The latest AME2016 compilation includes mass values for 46 additional nuclei in the  $^{40}\text{Ca}$ – $^{240}\text{U}$  region, and these are listed in Table I alongside predictions from various models. These include the “bare” models (i.e., before BNN refinement) HFB-19 [12], Duflo-Zuker [11], FRDM-2012 [18], HFB-27 [19], and WS3 [20]. Also shown are the predictions from the BNN-improved Duflo-Zuker and HFB-19 models [9]. The last column displays the total binding energy as reported in the AME2016 compilation [13]; quantities displayed in parentheses in the last three columns represent the associated errors. Note that we quote *differences* between the model predictions and the experimental masses using only the central values. Finally, the last row contains root-mean-square deviations associated with each of the models. The corresponding information in graphical form is also displayed in Fig. 1, but only for the five bare models discussed in the text.

The trends displayed in Table I and even more clearly illustrated in Fig. 1 are symptomatic of a well-known problem, namely, that theoretical mass models of similar quality that agree in regions where masses are experimentally known differ widely in regions where experimental data is not yet available [7]. Given that sensitivity studies suggest that resolving the  $r$ -process abundance pattern requires mass-model uncertainties of the order of  $\lesssim 100$  keV [21], the situation depicted in Fig. 1 is particularly dire. However, despite the large scattering in the model predictions, which worsens as one extrapolates

TABLE I. Theoretical predictions for the total binding energy of the 46 nuclei in the  $^{40}\text{Ca}$ - $^{240}\text{U}$  region that appear in the latest AME2016 [13] compilation but not in AME2012 [14]. The model predictions are relative to the new experimental values listed in the last column and the quantities in parentheses represent the associated error. The last row displays the root-mean-square deviation of each of the models. All quantities are given in MeV.

$Z$	$N$	HFB-19	DZ	FRDM-2012	HFB-27	WS3	HFB19-BNN	DZ-BNN	AME2016
20	33	1.959	3.476	4.571	2.169	1.370	1.948(1.520)	1.675(0.951)	441.521(0.044)
20	34	0.031	2.829	3.035	1.191	0.850	0.470(1.500)	0.840(0.880)	445.365(0.048)
21	35	-1.547	0.563	1.227	-0.777	-0.296	-0.216(0.928)	-0.226(0.686)	460.417(0.587)
21	36	-2.563	0.667	0.752	-1.473	-0.121	-0.953(0.975)	-0.117(0.611)	464.632(1.304)
24	40	-1.880	0.008	-0.872	-1.370	0.130	-0.130(0.793)	-0.192(0.498)	531.268(0.440)
25	37	-0.146	0.195	0.327	-0.106	0.549	0.555(1.060)	0.001(0.416)	529.387(0.007)
27	25	1.351	0.519	-0.274	-0.469	0.689	0.416(1.290)	0.141(0.650)	432.946(0.008)
29	27	2.564	0.188	0.199	-0.516	0.579	1.444(0.953)	0.460(0.513)	467.949(0.015)
30	52	-0.645	-1.697	-0.018	-0.315	-1.130	-0.505(0.896)	-0.498(0.638)	680.692(0.003)
32	54	-0.800	-1.143	0.338	-0.430	-0.596	-0.759(0.734)	-0.469(0.557)	718.498(0.438)
34	57	-0.279	-0.084	0.790	0.251	0.015	0.465(0.824)	0.297(0.504)	758.470(0.433)
37	63	0.768	-0.132	-1.038	-0.002	-0.846	1.144(0.886)	0.212(0.496)	824.432(0.020)
39	66	0.851	0.642	-0.293	1.211	0.788	0.555(0.868)	0.895(0.492)	868.247(1.337)
40	42	-0.718	-0.132	0.395	0.722	-0.092	-0.858(0.709)	-0.313(0.522)	694.185(0.011)
40	66	-0.239	-0.882	-1.344	0.051	-0.155	-0.581(0.826)	-0.671(0.536)	882.816(0.433)
40	67	0.191	-0.473	-0.823	0.751	0.525	-0.079(0.838)	-0.196(0.492)	886.717(1.122)
41	43	0.379	0.152	0.263	1.139	0.101	0.309(0.833)	0.018(0.531)	707.133(0.013)
41	69	0.011	-1.066	-1.091	0.471	-0.062	-0.014(0.855)	-0.583(0.501)	908.079(0.838)
43	71	-0.138	-1.003	-0.540	0.122	-0.532	0.141(0.731)	-0.290(0.522)	945.090(0.433)
43	72	-0.289	-0.494	-0.129	0.241	0.189	0.121(0.690)	0.441(0.495)	950.881(0.789)
45	76	-0.839	-0.930	-0.336	-0.539	0.161	-0.061(0.611)	0.175(0.510)	997.674(0.619)
46	77	-1.179	-0.794	-0.326	-0.919	-0.295	-0.420(0.651)	0.018(0.501)	1017.214(0.789)
48	81	-1.411	-0.911	-1.165	-1.351	-0.976	-0.458(0.801)	-0.560(0.444)	1066.705(0.017)
48	83	-1.750	-0.940	-1.141	-1.110	-0.720	-0.378(0.753)	-0.253(0.607)	1075.009(0.102)
51	87	-2.058	-0.724	0.133	-0.528	-0.872	-0.395(0.824)	-0.208(0.570)	1128.163(1.064)
53	88	-1.112	-0.281	0.498	-0.332	-0.138	-0.052(0.663)	0.034(0.596)	1156.518(0.016)
56	93	-0.899	-0.150	-0.415	-0.529	-0.157	-0.139(0.650)	-0.074(0.420)	1211.935(0.438)
57	93	-0.899	-0.520	-0.836	-0.579	-0.669	-0.501(0.715)	-0.677(0.398)	1222.234(0.435)
57	94	-1.209	-0.460	-0.745	-0.889	-0.635	-0.690(0.713)	-0.581(0.388)	1227.485(0.435)
63	74	-0.732	-0.680	-0.261	-0.052	0.340	-0.497(0.666)	-0.152(0.418)	1116.629(0.004)
81	109	-0.167	0.302	-0.298	-0.357	-0.149	-0.187(0.470)	-0.225(0.289)	1494.552(0.008)
82	133	-1.841	0.444	0.988	-0.061	0.200	-0.749(0.522)	0.257(0.317)	1666.838(0.052)
83	111	-0.269	0.764	0.000	-0.219	-0.506	-0.280(0.457)	0.247(0.301)	1516.930(0.006)
85	113	-0.244	0.736	0.076	-0.364	-0.162	-0.238(0.484)	0.225(0.304)	1538.336(0.006)
87	110	-0.443	0.995	0.061	-0.233	0.282	-0.287(0.680)	0.394(0.475)	1511.731(0.054)
87	111	-1.042	0.566	-0.347	-0.662	-0.141	-0.914(0.650)	0.016(0.404)	1520.483(0.032)
87	115	-0.144	0.293	0.126	-0.164	0.099	-0.113(0.571)	-0.215(0.317)	1559.246(0.007)
87	145	-1.391	1.367	0.099	-0.511	0.399	0.086(0.655)	0.144(0.421)	1758.409(0.014)
87	146	-1.538	1.850	0.183	-0.618	0.667	0.082(0.746)	0.426(0.586)	1763.633(0.020)
88	113	-0.426	0.712	0.311	-0.206	0.112	-0.320(0.712)	0.167(0.425)	1541.551(0.020)
89	116	0.075	0.042	0.354	0.215	0.271	0.153(0.739)	-0.473(0.389)	1570.884(0.051)
89	117	-0.438	-0.141	0.103	-0.018	0.149	-0.376(0.703)	-0.649(0.361)	1579.583(0.050)
92	123	0.408	0.268	-0.346	0.248	0.319	0.443(0.747)	-0.215(0.437)	1638.434(0.089)
92	124	0.375	0.505	-0.328	0.125	0.201	0.384(0.698)	0.005(0.456)	1648.362(0.028)
92	129	0.652	1.641	-0.285	0.622	0.095	0.504(0.677)	0.978(0.536)	1687.265(0.051)
92	130	0.639	1.399	-0.236	0.529	0.071	0.457(0.697)	0.713(0.531)	1695.584(0.052)
$\sigma_{\text{rms}}$		1.093	1.018	0.997	0.723	0.513	0.587	0.479	

further into the neutron drip lines, significant progress has been achieved in the last few years. Indeed, in the context of density functional theory, the HFB-27 mass model of Goriely, Chamel, and Pearson predicts a rather small rms deviation of  $\sim 0.5$  MeV for all nuclei with neutron and proton numbers larger than 8

[19]. Further, in the case of the Weizsäcker-Skyrme WS3 model of Liu, Wang, Deng, and Wu, the agreement with experiment is even more impressive: the rms deviation relative to 2149 known masses is a mere  $\sim 0.34$  MeV [20]. Although not as striking, the success of both models extends to their *predictions*

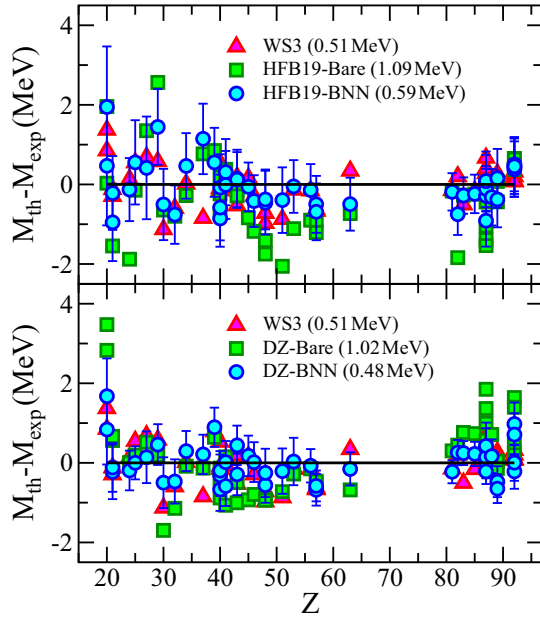


FIG. 2. Theoretical predictions for the total binding energy relative to experiment for the 46 nuclei in the  $^{40}\text{Ca}$ – $^{240}\text{U}$  region that appear in the latest AME2016 compilation but not in any of the earlier mass evaluations. The models shown include HFB-19 and Dufflo-Zuker together with their corresponding BNN refinements (shown with error bars). For reference the WS3 model of Liu and collaborators is also shown. Quantities in parentheses denote the rms deviations.

of the 46 new masses listed in Table I:  $\sigma_{\text{rms}} = 0.72$  MeV and  $\sigma_{\text{rms}} = 0.51$  MeV, respectively. This represents a significant improvement over earlier mass models that typically predict a rms deviation of the order of 1 MeV; see Table I and Fig. 1.

However, our main focus is to assess the improvement in the predictions of two of these earlier mass models (HFB-19 and DZ) as a result of the BNN refinement. In agreement with the nearly a factor-of-2 improvement reported in Ref. [9], we observe a comparable gain in the predictions of the 46 nuclear masses listed in Table I; that is,  $\sigma_{\text{rms}} = (1.093 \rightarrow 0.587)$  MeV and  $\sigma_{\text{rms}} = (1.018 \rightarrow 0.479)$  MeV for HFB-19 and DZ, respectively. Of course, an added benefit of the BNN approach is the supply of theoretical error bars. Indeed, when such error bars are taken into account—as we do in Fig. 2—then *all* of the refined predictions are consistent with the experimental values at the  $2\sigma$  level. For reference, also included in Fig. 2 are the impressive predictions of the WS3 model, albeit without any estimates of the theoretical uncertainties.

We close this section by addressing a particular set of nuclear masses that have been identified as “impactful” in sensitivity studies of the elemental abundances in  $r$ -process nucleosynthesis. These include a variety of neutron-rich isotopes in palladium, cadmium, indium, and tin; see Table I of Ref. [21]. As of today, none of these critical isotopes have been measured experimentally. However, many of them have been flagged (with the symbol #) in the AME2016 compilation to indicate that, while not strictly determined experimentally, the provided mass estimates were obtained from *experimental trends of neighboring nuclides* [13]. In Table II theoretical

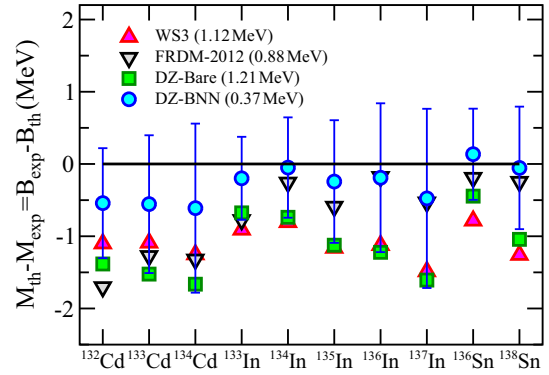


FIG. 3. Theoretical predictions for the total binding energy of those nuclei that have been identified as impactful in  $r$ -process nucleosynthesis [21]. All experimental values have been estimated from experimental trends of neighboring nuclides [13]. Quantities in parentheses denote the rms deviations.

predictions are displayed for those isotopes that have been both labeled as impactful and flagged. Predictions are provided for the WS3 [20], FRDM-2012 [18], DZ [11], and BNN-DZ [9] mass models. Root-mean-square deviations of the order of 1 MeV are recorded for all models, except for the improved Dufflo-Zuker model where the deviation is only 369 keV. This same information is depicted in graphical form in Fig. 3. The figure nicely encapsulates the spirit of our two-prong approach, namely, one that starts with a mass model of the highest quality (DZ) that is then refined via a BNN approach. The improvement in the description of the experimental data together with a proper assessment of the theoretical uncertainties are two of the greatest virtues of the BNN approach. Indeed, the BNN-DZ predictions are consistent with all masses of those impactful nuclei that have been determined from the experimental trends.

### III. CONCLUSIONS

Nuclear masses of neutron-rich nuclei are paramount to a variety of astrophysical phenomena ranging from the crustal composition of neutron stars [5,6,22–25] to the complexity of  $r$ -process nucleosynthesis [4,26,27]. Yet, despite enormous advances in experimental methods and tools, many of the masses of relevance to astrophysics lie well beyond the present experimental reach, leaving no option but to rely on theoretical extrapolations that often display large systematic variations. The current situation is particularly troublesome given that sensitivity studies require mass-model uncertainties to be reduced to about  $\lesssim 100$  keV in order to resolve  $r$ -process abundances.

There are at least two different approaches currently used to alleviate this problem. The first one consists of painstakingly difficult measurements near the present experimental limits that aim to inform and constrain mass models. The second approach is based on a global refinement of existing mass models through the training of an artificial neural network. This is the approach that we have advocated in this short contribution. Given that the training of the neural network

TABLE II. Theoretical predictions for the total binding energy relative to the experimental masses that have been estimated from experimental trends of neighboring nuclides [13] and that have been identified as impactful in  $r$ -process nucleosynthesis [21].

$Z$	$N$	WS3	FRDM	DZ	DZ-BNN	AME2016
48	84	-1.101	-1.704	-1.384	-0.542(0.761)	1078.176
48	85	-1.090	-1.273	-1.524	-0.556(0.954)	1079.827
48	86	-1.252	-1.322	-1.664	-0.611(1.170)	1082.988
49	84	-0.910	-0.775	-0.676	-0.198(0.574)	1092.595
49	85	-0.806	-0.256	-0.738	-0.049(0.695)	1094.914
49	86	-1.162	-0.590	-1.124	-0.243(0.849)	1097.820
49	87	-1.124	-0.178	-1.223	-0.190(1.030)	1099.832
49	88	-1.487	-0.531	-1.607	-0.476(1.240)	1102.439
50	86	-0.785	-0.190	-0.445	0.135(0.631)	1114.520
50	88	-1.259	-0.246	-1.043	-0.054(0.848)	1119.594
$\sigma_{\text{rms}}$		1.117	0.877	1.210	0.369	

relied exclusively on the AME2012 compilation, our approach was validated by comparing our theoretical predictions against the new information provided in the most recent AME2016 compilation.

The comparison against the newly available AME2016 data was highly successful. For the nearly 50 new mass measurement reported in the  $^{40}\text{Ca}$ – $^{240}\text{U}$  region, the rms deviation of the two BNN-improved models explored in this work (Duflo-Zuker and HFB-19) was reduced by nearly a factor of 2 relative to the unrefined bare models. Further, for the masses of several impactful isotopes for the  $r$ -process, the predictions from the improved Duflo-Zuker model were fully consistent with the new AME2016 estimates and in far better agreement than some of the most sophisticated mass models available in the literature. As important, all nuclear-mass predictions in the BNN approach incorporate properly estimated statistical uncertainties. When these theoretical error bars are incorporated, then *all* of our predictions are consistent with experiment at the  $2\sigma$  level.

Ultimately, improvements in mass models require a strong synergy between theory and an experiment. Next-generation rare-

isotope facilities will produce new exotic nuclei that will help constrain the physics of weakly bound nuclei. In turn, improved theoretical models will suggest new measurements on a few critical nuclei that will best inform nuclear models. We are confident that the BNN approach advocated here will play a critical role in this endeavor, particularly in identifying those nuclei that have the strongest impact in resolving some outstanding questions in nuclear astrophysics. We are hopeful that in the near future mass-model uncertainties—both statistical and systematic—will be reduced to less than 100 keV, which represents the elusive standard required to resolve the  $r$ -process abundance pattern.

#### ACKNOWLEDGMENTS

We are thankful to P. Giuliani for many stimulating discussions. This material is based upon work supported by the US Department of Energy Office of Science, Office of Nuclear Physics under Grant No. DE-FG02-92ER40750.

- [1] Nuclear Science Advisory Committee, *Reaching for the Horizon; The 2015 Long Range Plan for Nuclear Science* (US Department of Energy, Washington, 2015).
- [2] National Research Council, *Nuclear Physics: Exploring the Heart of Matter* (The National Academies Press, Washington, 2012).
- [3] National Research Council, *Connecting Quarks with the Cosmos: Eleven Science Questions for the New Century* (The National Academies Press, Washington, 2003).
- [4] M. R. Mumpower, R. Surman, G. C. McLaughlin, and A. Aprahamian, *Prog. Part. Nucl. Phys.* **86**, 86 (2016).
- [5] X. Roca-Maza and J. Piekarewicz, *Phys. Rev. C* **78**, 025807 (2008).
- [6] R. Utama, J. Piekarewicz, and H. B. Prosper, *Phys. Rev. C* **93**, 014311 (2016).
- [7] K. Blaum, *Phys. Rep.* **425**, 1 (2006).
- [8] R. Utama, W.-C. Chen, and J. Piekarewicz, *J. Phys. G: Nucl. Part. Phys.* **43**, 114002 (2016).
- [9] R. Utama and J. Piekarewicz, *Phys. Rev. C* **96**, 044308 (2017).
- [10] P. Möller, J. R. Nix, W. D. Myers, and W. J. Swiatecki, *At. Data Nucl. Data Tables* **59**, 185 (1995).
- [11] J. Duflo and A. P. Zuker, *Phys. Rev. C* **52**, R23(R) (1995).
- [12] S. Goriely, N. Chamel, and J. M. Pearson, *Phys. Rev. C* **82**, 035804 (2010).
- [13] W. J. Huang, G. Audi, M. Wang, F. G. Kondev, S. Naimi, and X. Xu, *Chin. Phys. C* **41**, 030002 (2017).
- [14] M. Wang, G. Audi, A. Wapstra, F. Kondev, M. MacCormick, X. Xu, and B. Pfeiffer, *Chin. Phys. C* **36**, 1603 (2012).
- [15] R. Neal, *Bayesian Learning of Neural Network* (Springer, New York, 1996).
- [16] D. J. MacKay, *Nucl. Instrum. Methods Phys. Res., Sect. A* **354**, 73 (1995).
- [17] D. J. MacKay, *Neural Comput.* **11**, 1035 (1999).
- [18] P. Möller, W. D. Myers, H. Sagawa, and S. Yoshida, *Phys. Rev. Lett.* **108**, 052501 (2012).

- [19] S. Goriely, N. Chamel, and J. M. Pearson, *Phys. Rev. C* **88**, 061302(R) (2013).
- [20] M. Liu, N. Wang, Y. Deng, and X. Wu, *Phys. Rev. C* **84**, 014333 (2011).
- [21] M. R. Mumpower, R. Surman, D. L. Fang, M. Beard, P. Moller, T. Kawano, and A. Aprahamian, *Phys. Rev. C* **92**, 035807 (2015).
- [22] G. Baym, C. Pethick, and P. Sutherland, *Astrophys. J.* **170**, 299 (1971).
- [23] P. Haensel, J. L. Zdunik, and J. Dobaczewski, *Astron. Astrophys.* **222**, 353 (1989).
- [24] P. Haensel and B. Pichon, *Astron. Astrophys.* **283**, 313 (1994).
- [25] S. B. Rüster, M. Hempel, and J. Schaffner-Bielich, *Phys. Rev. C* **73**, 035804 (2006).
- [26] G. Wallerstein, I. Iben, P. Parker, A. M. Boesgaard, G. M. Hale, A. E. Champagne *et al.*, *Rev. Mod. Phys.* **69**, 995 (1997).
- [27] I. Petermann, G. Martínez-Pinedo, A. Arcones, W. R. Hix, A. Keli, K. Langanke, I. Panov, T. Rauscher, K.-H. Schmidt, F.-K. Thielemann, and N. Zinner, *J. Phys.: Conf. Ser.* **202**, 012008 (2010).